High-resolution broadband (>100 cm^{-1}) infrared heterodyne spectro-radiometry using an external cavity quantum cascade laser

Damien Weidmann,[1,*] Gerard Wysocki[2,]**

[1]*Space Science and Technology Department, STFC Rutherford Appleton Laboratory, Harwell Science and Innovation Campus, Didcot, Oxfordshire, OX11 0QX, UK*
[2]*Electrical Engineering Department, Princeton University, Princeton, NJ, 08544, USA*
* damien.weidmann@stfc.ac.uk; ** gwysocki@princeton.edu

Abstract: Broadband thermal infrared heterodyne spectro-radiometry using an external cavity quantum cascade laser as a tunable local oscillator has been performed over a frequency range of more than 100 cm^{-1} at a central frequency of 1190 cm^{-1}. Heterodyne spectro-radiometry is demonstrated for two local oscillator tuning modes: broadband tuning for transmission and emission spectroscopy of broadband absorbers (Freon 12), and broadband frequency selection in combination with fine continuous frequency tuning for high-resolution (0.021 cm^{-1}) transmission spectroscopy (N_2O). In each case concentration retrievals are performed and analyzed. The spectro-radiometer noise level is demonstrated to be twenty two and eight times the fundamental shot-noise limit in the two scanning modes respectively.

OCIS codes: (300.6310) Spectroscopy heterodyne; (300.6390) Spectroscopy molecular; (140.3600) Lasers tunable; (280.4991) Passive remote sensing.

References and links

1. R.T. Menzies, "Laser heterodyne detection techniques," in *Laser monitoring of the atmosphere, Springer-Verlag Topics in Appl. Phys.* **14**, ed E. D. Hinkley, 297 (1976).
2. A. Betz, E. C. Sutton, and R. A. McLaren, "Infrared Heterodyne Spectroscopy in Astronomy," in Laser Spectroscopy III, Springer Series in *Optical Sciences* **7**, eds J. L. Hall and J. L. Carlsten, 31 (1977).
3. R. T. Menzies and M. S. Shumate, "Air Pollution: Remote Detection of Several Pollutant Gases with a Laser Heterodyne Radiometer," Science **184**, 570-572 (1974).
4. J. Faist, F. Capasso, D. L. Sivco, C. Sirtori, A. L. Hutchinson, and A. Y. Cho, "Quantum Cascade Laser," Science **264**, 553-556 (1994).
5. Y. Bai, S. R. Darvish, S. Slivken, W. Zhang, A. Evans, J. Nguyen, and M. Razeghi,"Room temperature continuous wave operation of quantum cascade lasers with watt-level optical power," Appl. Phys. Lett. **92**, 101105 (2008).
6. L. Zhijun, D. Wasserman, S. S. Howard, A. J. Hoffman, C. F. Gmachl, W. Xiaojun, T. Tanbun-Ek, C. Liwei, and C. Fow-Sen,"Room-temperature continuous-wave quantum cascade lasers grown by MOCVD without lateral regrowth," IEEE Photon. Technol. Lett. **18**, 12, 1347-1349 (2006).
7. G. Sonnabend, D. Wirtz, and R. Schieder, "Evaluation of quantum-cascade lasers as local oscillators for infrared heterodyne spectroscopy," Appl. Opt. **44**, 7170-7172 (2005).
8. D. Weidmann, W. J. Reburn, and K. M. Smith, "Ground-based prototype quantum cascade laser heterodyne radiometer for atmospheric studies," Rev. Sci. Instrum. **78**, 073107 (2007).
9. A. Wittmann, T. Gresch, E. Gini, L. Hvozdara, N. Hoyler, M. Giovannini, and J. Faist, "High-Performance Bound-to-Continuum Quantum-Cascade Lasers for Broad-Gain Applications," IEEE J. Quantum Electron. **44**, 36-40 (2008).
10. G. Wysocki, R. Lewicki, R. F. Curl, F. K. Tittel, L. Diehl, F. Capasso, M. Troccoli, G. Hofler, D. Bour, S. Corzine, R. Maulini, M. Giovannini, and J. Faist, "Widely tunable mode-hop free external cavity quantum cascade lasers for high resolution spectroscopy and chemical sensing," Appl. Phys. B **92**, 305-311 (2008).
11. A. Mohan, A Wittmann, A. Hugi, S Blaser, M. Giovannini, and J. Faist, "Room-temperature continuous-wave operation of an external-cavity quantum cascade laser," Opt Lett. **32**, 2792-2794 (2007).

#104097 - $15.00 USD Received 17 Nov 2008; revised 20 Dec 2008; accepted 22 Dec 2008; published 24 Dec 2008

12. R. Lewicki, G. Wysocki, A. A. Kosterev, and F. K. Tittel, "QEPAS based detection of broadband absorbing molecules using a widely tunable, cw quantum cascade laser at 8.4 μm," Opt. Express **15**, 7357-7366 (2007).
13. M. C. Phillips and N. Ho,"Infrared hyperspectral imaging using a broadly tunable external cavity quantum cascade laser and microbolometer focal plane array," Opt. Express **16**, 1836-1845 (2008).
14. D. Stupar, J. Krieg, P. Krötz, G. Sonnabend, M. Sornig, T. F. Giesen, and R. Schieder,"Fully reflective external-cavity setup for quantum-cascade lasers as a local oscillator in mid-infrared wavelength heterodyne spectroscopy," Appl. Opt. **47**, 2993-2997 (2008).
15. D. Weidmann, K. Smith, and B. Ellison, "Experimental investigation of high-frequency noise and optical feedback effects using a 9.7 μm continuous-wave distributed-feedback quantum cascade laser," Appl. Opt. **46**, 947-953 (2007).
16. C. Rodgers, "Inverse methods for atmospheric sounding: theory and practice," World Scientific (2000).
17. S. W. Sharpe, T. J. Johnson, R. L. Sams, P. M. Chu, G. C. Rhoderick, and P. A. Johnson, "Gas-Phase Databases for Quantitative Infrared Spectroscopy," Appl. Spectrosc. **58**, 1452-1461 (2004).
18. L. S. Rothman, D. Jacquemart, A. Barbe, D. Chris Benner, M. Birk, L. R. Brown, M. R. Carleer, C. Chackerian, K. Chance, L. H. Coudert, V. Dana, V. M. Devi, J.-M Flaud, R. R. Gamache, A. Goldman, J.-M. Hartmann, K. W. Jucks, A. G. Maki, J.-Y. Mandin, S. T. Massie, J. Orphal, A. Perrin, C. P. Rinsland, M. A. H. Smith, J. Tennyson, R. N. Tolchenov, R. A. Toth, J. Vander Auwera, P. Varanasi, and G. Wagner, "The HITRAN 2004 molecular spectroscopic database," J. Quant. Spectrosc. Radiat. Transfer **96**, 139–204 (2005).
19. D. Weidmann, W. J. Reburn, and K. M. Smith, "Retrieval of atmospheric ozone profiles from an infrared quantum cascade laser heterodyne radiometer: results and analysis," Appl. Opt. **46**, 7162-7171 (2007).
20. G. Wysocki, R. F. Curl, F. K. Tittel, R. Maulini, J. M. Bulliard, and J. Faist, "Widely tunable mode-hop free external cavity quantum cascade laser for high resolution spectroscopic applications," Appl. Phys. B **81**, 769–777 (2005).

1. Introduction

Laser heterodyne radiometers (LHRs) operating in the thermal infrared (IR), provide high resolving power (more than 10^6) combined with high sensitivity (shot-noise limited) and a very small field of view. These characteristics make IR LHR instruments well suited to atmospheric remote sensing of compounds at low pressure, meaning those found in the upper troposphere, the stratosphere and at higher altitudes [1]. Similarly IR LHR instruments have great potential for astronomy and planetary remote sensing applications [2].

Thermal IR laser heterodyne systems were pioneered using CO_2 lasers as optical local oscillators (LO) [3]. The development of mid-infrared quantum cascade lasers (QCLs) [4] has offered new opportunities for IR LHR developments. QCLs exhibit high continuous wave output power (50 mW and above), single mode emission, and continuous frequency tunability. In addition they operate at room temperature, and have the size of a semiconductor chip, making them well suited for the development of compact and robust laser based instruments [5, 6]. Therefore QCLs possess ideal characteristics to be used as optical LO in heterodyne systems [7, 8].

LHR instruments based on single mode distributed feedback (DFB) QCLs are restricted in terms of frequency selection and tunability to about 1% of the laser central frequency through thermal tuning of the intra-cavity index of refraction. Extending the LO frequency tuning range is desirable to increase the flexibility of LHR instruments by allowing multi-species monitoring and broadband absorber/emitter characterization. The intrinsic gain curve of QCLs, especially those based on bound-to-continuum transitions, is spectrally broad [9] but the implementation of DFB structure for single mode operation considerably restricts the laser tuning range. An external cavity configuration aims to obviate this particular DFB limitation by introducing a tunable spectral filter which does not compromise the use of the full QCL gain bandwidth. Recently external cavity QCL (EC-QCL) systems have been brought to maturity: room temperature, continuous wave mode operation covering more than 15% of the laser central frequency in the mid infrared has been successfully demonstrated [10, 11]. As with mid-IR photoacoustic spectroscopy [12] or hyperspectral imaging systems [13], the use of EC-QCLs is a way to increase the spectral operating range and molecular detection

#104097 - $15.00 USD Received 17 Nov 2008; revised 20 Dec 2008; accepted 22 Dec 2008; published 24 Dec 2008

capabilities of LHR instruments. The first EC-QCL LHR system covering 30 cm^{-1} has recently been reported [14].

In this paper a thermal infrared LHR based on a Littrow EC-QCL is presented and demonstrated. Heterodyne detection covering a spectral range of over 100 cm^{-1} around 1190 cm^{-1} has been performed. The widely tunable LHR is demonstrated through two separate operating modes: a broadband tuning mode with low frequency sampling resolution (~0.5 cm^{-1}) using only coarse grating tuning and a high-resolution (~0.001 cm^{-1}) tuning mode where broadband coverage and mode-hop-free wavelength tuning are used in combination. Dichlorodifluoromethane (Freon 12) and nitrous oxide (N_2O) have been used as target molecules respectively to test the performance and demonstrate the capabilities of the EC-QCL LHR instrument.

The experimental details are given in the first section. The second section is dedicated to broadband absorption and emission measurements of Freon 12. High-resolution N_2O absorption measurements are presented in section 3. The final sections contain details of the analysis performed to retrieve gas concentrations and conclusions.

2. Experimental details

The local oscillator used in these experiments was an EC-QCL in the Littrow configuration. The gain curve of the Fabry-Perot QCL chip was centered at 8.4 µm (1190 cm^{-1}) and could provide up to ~180 cm^{-1} tunability when operated at -30°C. The EC-QCL system has already been fully described in Ref. 10. In summary, anti-reflection and high reflection coatings were deposited on the front and back facets of the QCL chip respectively. Collimation and EC coupling were ensured by an anti-reflection coated germanium aspheric lens (24 mm diameter, f/0.6). The first-order reflection from the grating (~45° blaze angle, 135 lines per millimeter) was sent back into the laser chip to provide wavelength selective laser feedback. The laser output is formed by the zeroth-order reflection. The EC-QCL was capable of narrowband high-resolution mode-hop-free wavelength tuning anywhere within the entire tuning range. In this mode piezo-electric actuators controlled the grating angle and the extended cavity length. The laser injection current was synchronously scanned with the grating angle and the cavity length for passive laser mode tracking. The EC opto-mechanical design was optimized to provide a stable output beam axis (fixed direction, no walk-off) during the tuning process. The laser was thermoelectrically cooled, and was operated in the temperature range of -15 to 0 °C, which allowed up to ~135 cm^{-1} tunability.

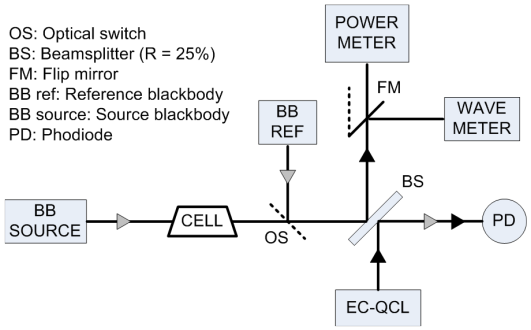

Fig. 1. Schematic optical layout of the external cavity quantum cascade laser heterodyne spectro-radiometer.

The EC-QCL was integrated as the LO with the LHR as shown schematically in Fig. 1. The experimental configuration was similar to the one reported and fully characterized in Ref. 8. 25% of the LO output radiation was directed to a high speed Mercury Cadmium Telluride (HgCdTe) photodiode (photomixer) and the remaining 75% was transmitted through

#104097 - $15.00 USD Received 17 Nov 2008; revised 20 Dec 2008; accepted 22 Dec 2008; published 24 Dec 2008

a beam splitter towards either a power meter, or a wavemeter which monitored the laser frequency with an accuracy of 0.001 cm^{-1}. Incoherent radiation within the field of view of the instrument is mixed with the coherent LO beam at the photomixer. Two different configurations were possible: a) a transmission configuration in which the radiation from a blackbody source was directed through an absorption cell and detected by the LHR, and b) an emission configuration in which thermal radiation from gas molecules in the cell was detected. In both configurations, the LHR was sensitive to the brightness contrast between the target and a reference blackbody shown in the optical layout in Fig. 1.

For clarity the individual optical components are not represented in Fig. 1. With the exception of the beamsplitter and the laser collimating lens, all optical elements were reflective to reduce spurious optical feedback and to ensure a fully achromatic optical system which could accommodate the broad frequency range of the EC-QCL LHR.

The heterodyne signal collected from the photodiode output was amplified using two 30 dB Avantek voltage amplifiers, filtered (lumped components filters), and detected by a radio-frequency (RF) detector (Herotek Schottky diode). The filtering stage defines the LHR spectral resolution as well as the instrument lineshape (ILS). After RF detection the signal was measured by a lock-in amplifier referenced to the optical switch frequency. The subsequent acquisition was made by a computer equipped with Labview software and a National Instruments data acquisition card.

Gas samples were directly prepared in absorption cells by mixing pure gas samples with ambient air in a simple and manually operated three way gas handling system. Uncalibrated pressure gauges (1000 mbar Baratron manometer) were used to estimate the prepared mixture concentration. The relative concentration accuracy obtained with this method is believed to be no better than 30%.

3. Broadband absorber spectro-radiometry

To demonstrate the capability of the broadly tunable EC-QCL LHR, Freon 12 (dichlorodifluoromethane, CCl_2F_2) was chosen as broadband absorber/emitter. At atmospheric pressure Freon 12 exhibits a 30 cm^{-1} wide absorption band, centered at 1160 cm^{-1} which corresponds to the asymmetric stretch of the CF_2 group. This band also exhibits a strong Q branch with narrow spectral features.

A 0.5% mixture of Freon 12 in air at atmospheric pressure was injected into a 51±1 mm long gas cell. Spectro-radiometric measurements were made with the gas cell positioned as shown in Fig. 1.

3.1 Transmission

The broadband frequency scan of the LO was performed by varying the EC-QCL grating angle. The laser injection current and laser temperature were held constant (at 650 mA and -5°C respectively) whilst the grating angle was changed using a computer-controlled rotation stage. The external cavity length was not controlled during this mode of operation, and the EC-QCL operated on modes exhibiting the lowest losses. Consequently the EC-QCL tended to lase at frequencies separated by the free spectral range of the residual cavity formed by the Fabry Perrot QCL gain medium (~0.55 cm^{-1}) within the diffraction grating bandwidth (~0.85 cm^{-1} approximated as twice the resolving power for a beam diameter of 20 mm). Experimental verification of the frequency sampling resolution was performed using wavemeter readings (see Fig. 2) and high-resolution motor steps. This yielded an average mode-hop size of 0.58 cm^{-1}, which is in excellent agreement with the theoretical value. Figure 2 shows the mode-hops between EC longitudinal modes, which are separated by ~0.07cm^{-1}. Also the laser frequency tuning slope of 3×10^{-5} cm^{-1}/step is apparent, due to the variation of the EC length during the rotation of the grating. However these effects were negligible when 0.58cm^{-1} wide step tuning was performed.

#104097 - $15.00 USD Received 17 Nov 2008; revised 20 Dec 2008; accepted 22 Dec 2008; published 24 Dec 2008

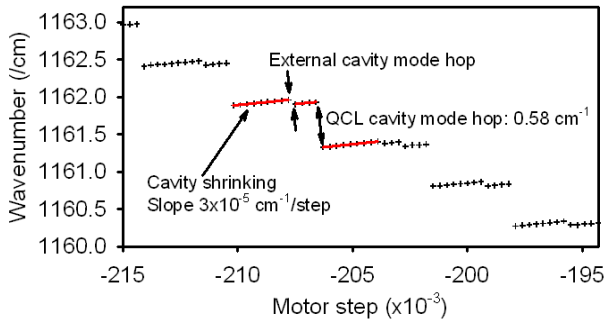

Fig. 2. Wavelength calibration of a coarse grating angle scan using wavemeter readings and high-resolution motor steps. Without EC length and QCL current control the frequency sampling resolution is limited to 0.58 cm^{-1}.

The motor step resolution was then adjusted accordingly, and a prior calibration of the grating motor position with respect to the actual laser frequency was carried out using the wavemeter. Using this method, spectra with absolute frequency calibration were recorded.

In this mode the full photomixer bandwidth could be used without compromising the spectral resolution of the LHR. The excess noise from the EC-QCL was directly measured with an RF spectrum analyzer and the corresponding noise power referenced to the noise level of the photomixer is shown in Fig. 3. The most significant contribution of the laser excess noise is observed at frequencies below 200 MHz. A high pass filter with a cutoff frequency of 300 MHz was used to reject low frequency noise [15]. This yielded an effective double side band LHR resolution of 2840 MHz (0.095 cm^{-1}).

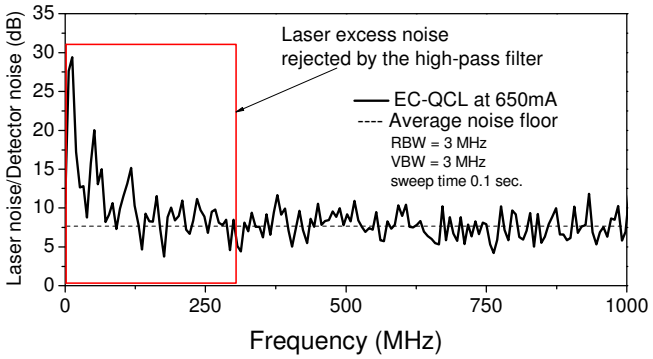

Fig. 3. EC-QCL excess RF noise measured relatively to the photomixer noise using an RF spectrum analyzer.

For transmission measurements, a high-temperature blackbody was used as a background source radiating through the absorption cell. The temperature of this source blackbody was set to 823.15 K. Ambient radiation was used as a reference. LHR settings were adjusted as follows: the integration time was 1s, switching frequency between the source and the reference radiation was 2.17 kHz, and 500 points were acquired within the complete wavelength scan. The laser power varied during the scan, this is primarily related to the spectral envelope of the laser gain curve. Consequently, LO power modulation was observed within the spectrum. The laser power received by the photomixer varied from 3.3 mW at high frequency (1190 cm^{-1}, close to the laser gain peak) to 2.4 mW at low frequency (1135 cm^{-1}). The LO power was adjusted so that it never exceeded the saturation level of the photomixer.

#104097 - $15.00 USD Received 17 Nov 2008; revised 20 Dec 2008; accepted 22 Dec 2008; published 24 Dec 2008

The observed Freon 12 heterodyne transmission spectrum spanning 60 cm^{-1} is shown in Fig. 4.

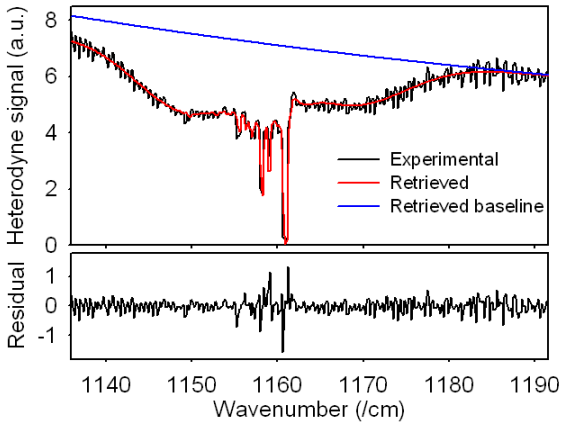

Fig. 4. An approximately 60 cm^{-1} wide heterodyne transmission spectrum of a 0.5% mixture of Freon 12 in air at atmospheric pressure. The retrieved spectrum and the retrieved baseline are also plotted. The lower plot shows the residual between the measured spectrum and the fit.

To compare the experimental heterodyne spectrum with the spectral database, we developed a non linear Levenberg-Marquardt algorithm, based on the optimal estimation method (OEM) [16]. The forward model used the reference composite spectrum of Freon 12 included in the Pacific Northwest National Laboratory (PNNL) spectral database [17]. The forward model can be written as:

$$F(k,a,b,c,\sigma) = 10^{-A(\sigma)\cdot k} \cdot (a + b\sigma + c\sigma^2), \quad (1)$$

where A(σ) is the composite reference absorbance spectrum after path-concentration normalization, k is the unknown path-concentration parameter (in ppm-m), a, b, c are polynomial coefficients to be retrieved, which describe the spectral shape of the baseline. The baseline variation was mainly related to the LO power modulation occurring during the scan and to a lesser extent the blackbody curve of the radiation source, which starts to be significant over such a wide frequency range. The ILS has not been taken into account in the forward model as it does not have any significance given the relatively low sampling resolution and the relatively large spectral width of the Freon 12 absorption features. The base 10 exponential appearing in Eq. (1) is related to the definition of the PNNL reference data. The relative uncertainties on a priori parameters were chosen to be 100%.

The upper panel in Fig. 4 shows the measured spectrum with the 'best-fit' calculated spectrum superimposed. Also shown is the retrieved baseline. The lower panel in Fig. 4 shows the fit residual. The measured and retrieved spectra match extremely well. It is apparent in Fig. 4 that there are some discrepancies between the measured and calculated spectra around the narrow Q-branch features. This is primarily due to the limited frequency sampling resolution shown in Fig. 2, which results in an uncertainty in the frequency axis calibration of 0.58 cm^{-1} and is related to mode-hopping. This has greatest effect around the slopes of narrow spectral features. In Fig. 4, the retrieved value of the path-concentration parameter is 227±7 ppm-m, corresponding to a Freon 12 concentration of 0.45±0.03% (including the uncertainty of the gas cell path length which represent 40% of the full uncertainty).

To further analyze the performance of the EC-QCL LHR, a baseline scan was recorded under the same conditions. The resulting spectrum is shown in Fig. 5, along with a quadratic correction retaining only the noise. The radiation power difference observed with the LHR and averaged over the scan corresponds to 3.62 pW. The noise (standard deviation)

#104097 - $15.00 USD Received 17 Nov 2008; revised 20 Dec 2008; accepted 22 Dec 2008; published 24 Dec 2008

corresponds to 0.11 pW which is 22 times higher than the theoretical ultimate shot noise limit, given a photomixer with a 25% heterodyne efficiency. This noise value was subsequently used to quantify the measurement noise in the retrieval algorithm.

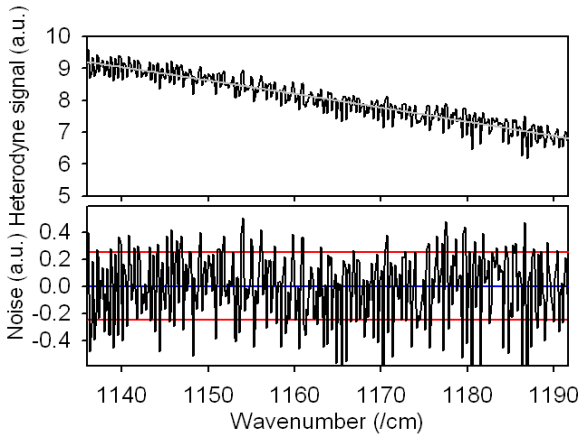

Fig. 5. Record of the baseline variation within approximately 60 cm^{-1} for experimental noise estimation. The lower panel shows the baseline after correction with a quadratic function. The horizontal lines indicate the standard deviation of measurements.

The regular structures clearly visible in the baseline scan are a major contribution to this excess noise. It has been shown previously [15] that LHR systems using continuously tunable laser LOs suffer significant performance degradation if spurious optical feedbacks are not controlled.

EC-QCLs in the Littrow configuration, with the device output formed by the zeroth order grating reflection, are generally less sensitive to uncontrolled optical feedback to the gain medium than DFB QCLs for two reasons. Firstly, the grating nearly suppresses the coupling of retro-reflected stray light back to the cavity since the coupling efficiency is approximately 5%. Secondly, feedback is further reduced by the coupling efficiency of the intra-cavity collimating optics, which is approximately 30%.

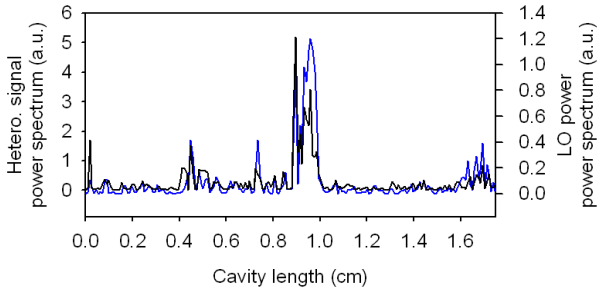

Fig. 6. Power spectra of the heterodyne noise (black line) and the LO power noise (blue line). The abscissa has been calibrated in terms of the Fabry-Perot cavity length.

To investigate the origin of the regular patterns in the noise spectrum, shown in Fig. 5, a Fourier transform of the baseline scan was calculated and is shown as a function of the characteristic Fabry-Perot cavity length in Fig. 6. During the broad LO frequency scan, the LO power was simultaneously recorded and the results of a similar cavity-length analysis are also shown in Fig. 6. Highly correlated specific cavity length resonances can be observed in both traces. The strongest component around ~0.95 cm corresponds to the QCL gain medium

#104097 - $15.00 USD Received 17 Nov 2008; revised 20 Dec 2008; accepted 22 Dec 2008; published 24 Dec 2008

optical cavity length. Information about spurious reflections from longer cavities external to the laser could not be obtained due to the limited frequency scan sampling resolution. The strong correlation between the two traces in Fig. 6 suggests that heterodyne signal variations are primarily related to LO power modulation.

3.2 Emission

The EC-QCL LHR was operated in the sample emission mode, in an attempt to measure intrinsic emission from the Freon 12 contained in the cell. This experiment was conducted using another laser chip with slightly different tuning characteristics but targeting the same spectral feature. The QCL was coupled to the external cavity and operated with a drive current of 700 mA and temperature of -5°C.

Sample emission measurements at room temperature are challenging as the brightness levels are low and comparable to the background. A mixture of 2% Freon 12 with air at atmospheric pressure was prepared and injected into the 51 mm gas cell. The source blackbody was set to 263.15 K to provide contrast against the room-temperature gas sample. The reference blackbody was set to 100 K. The time constant was increased to 5 s, and 200 data points spanning approximately 100 cm^{-1} were acquired by varying the LO grating angle alone. The acquired heterodyne emission spectrum is shown in the upper panel of Fig. 7. The room-temperature Freon 12 emission is clearly visible over the baseline. As expected the signal-to-noise ratio is low relative to the transmission measurement due to the low brightness.

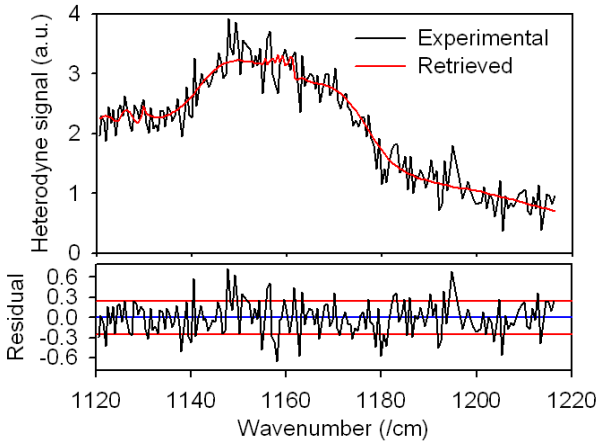

Fig. 7. A 100 cm^{-1} wide heterodyne emission spectrum of 2% Freon 12 in air at atmospheric pressure, contained in a 51 mm long gas cell.

Information was retrieved from the emission spectrum with the same OEM algorithm used in the analysis of the transmittance measurement, but with a different forward model: in this case the isothermal radiative transfer equation was used, with a second order polynomial baseline correction:

$$F(k,a,b,c,\sigma) = \left[B_0(\sigma)\cdot 10^{-A(\sigma)\cdot k} + B_A(\sigma)\cdot(1-10^{-A(\sigma)\cdot k})\right]\times(a+b\sigma+c\sigma^2), \quad (2)$$

where B_0 and B_A are the Planck brightness values of the source and ambient temperature blackbodies respectively.

The 'best-fit' synthetic spectrum is superimposed on the measurement in Fig. 7, with the corresponding residual shown in the lower panel.

The retrieved path-concentration parameter was 1065±154 ppm-meter, corresponding to a Freon 12 concentration of 2.1±0.4%. Even though the retrieved value is very close to what was expected, the retrieval results suggest a more thorough analysis. Indeed, the laser used in

#104097 - $15.00 USD Received 17 Nov 2008; revised 20 Dec 2008; accepted 22 Dec 2008; published 24 Dec 2008

this measurement exhibited a very strong non-linear power modulation during the scan (the c parameter in the forward model) which decreased confidence in the retrieved value of k. In other words, c and k are not independent enough to draw a firm conclusion on the retrieved value of k. An example of retrieval analysis illustrating a similar issue is given in section 5.

4. High-resolution transmission spectroscopy

To demonstrate the high-resolution capability of the EC-QCL LHR, spectroscopy of low-pressure nitrous oxide (N_2O) was chosen. N_2O is a linear molecule exhibiting a ro-vibrational spectrum with well separated and intense absorption lines. Typical line intensities within the tuning range of the EC-QCL are greater than 10^{-20} $cm^{-1}/(molec.cm^{-2})$ [18]. These intense transitions belong primarily to the ν_1 and $2\nu_2$ bands.

In the high-resolution mode, the external grating is tuned so that the LO frequency coarsely coincides with a selected N_2O line. Then, fine frequency tuning is achieved through simultaneous modulation of the laser current, the grating angle and the extended cavity length. The laser drive current and temperature were set to 650 mA and -5°C respectively. A sinusoidal current modulation of 78 mA peak-to-peak was applied to the QCL to perform the fine frequency sweep. Grating tuning and cavity length modulation were performed using piezo actuators. The LHR was operated in the transmission mode, with the source blackbody temperature set to 823.15 K and the reference blackbody at ambient temperature. A mixture of 25% N_2O in air, at 125 mbar total pressure, was prepared and injected into the cell. A 320 MHz bandpass filter centered at 700 MHz was used to set the double side band resolution of the instrument to 0.021 cm^{-1}. The integration time constant was set to 100 ms.

Figure 8 summarizes a set of four high-resolution spectra recorded within a spectral range greater than 100 cm^{-1}. The bottom panel in the figure shows N_2O transitions taken from the HITRAN 2004 database [18]. The EC-QCL was sequentially set to central frequencies of 1150.9, 1183.5, 1237.8, and 1253.5 cm^{-1}. At each frequency a mode-hop-free scan was applied to record the high-resolution heterodyne transmission spectrum of the individual N_2O line.

Each of the spectra shown in Fig. 8 was used to retrieve the N_2O concentration using the OEM algorithm. The forward model was based on the Beer-Lambert law. The HITRAN 2004 database and Voigt line profiles were used for the line-by-line calculation of the theoretical transmission spectrum. The forward model included a quadratic baseline, a frequency offset parameter and the total gas pressure. When operating at high spectral resolution the LHR ILS must also be considered: it was precisely measured and incorporated to the forward model [19]. The effect of the ILS can clearly be seen in the transmission spectra, where single absorption lines are transformed into doublets due to convolution with the double-sideband ILS. The absorption line appearing in spectrum 4 in Fig. 8 is very intense and saturates. Consequently the linewidth is broader than the ILS and the doubling effect does not appear.

Experimental data were recorded and processed in the following sequence:

- The LO frequency was coarsely tuned to the chosen N_2O line frequency through grating angle adjustment.
- The N_2O cell was replaced by a germanium etalon with a 0.048 cm^{-1} free spectral range. Etalon fringes were recorded during a mode-hop free fine frequency scan. Fringe peak detection was used to provide a relative frequency calibration of the laser scan. This was necessary due to the sinusoidal LO frequency tuning (piezo-electric actuators are driven with sinusoidal waveform), causing spectra to be recorded on an irregular abscissa grid.
- A baseline measurement was also made to provide a priori parameters for the forward model (a, b, and c).
- The N_2O cell was reinserted in the optical path and a heterodyne transmission spectrum was recorded.
- The retrieval of the path-concentration parameter was performed. Typically convergence was achieved in about ten iterations with a normalized χ^2 parameter of approximately 0.1.

#104097 - $15.00 USD Received 17 Nov 2008; revised 20 Dec 2008; accepted 22 Dec 2008; published 24 Dec 2008

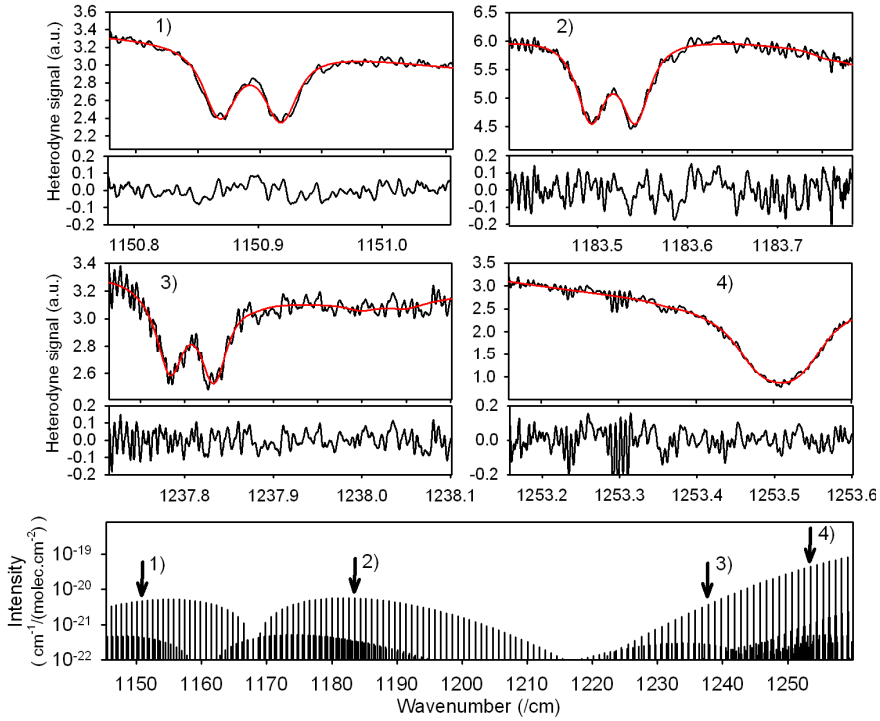

Fig. 8. Four high resolution transmission spectra of N_2O lines located within the 1150-1260 cm^{-1} range. Measurements (black line) and retrieved synthetic spectra (red line) are shown. The bottom panel shows the HITRAN 2004 N_2O absorption line intensities located within the EC-QCL tuning range. Arrows indicate where the laser central frequency was set to perform continuous fine tuning.

In Fig. 8 'best-fit' calculated spectra are superimposed on the measurements and in each case the corresponding residuals are given below. Table 1 summarizes the spectroscopic parameters of the N_2O lines shown in Fig. 8 [18]. The last column gives the retrieved N_2O concentrations and their associated standard deviations taken from the covariance matrix.

Table 1. The spectroscopic parameters of the four N_2O lines shown in Fig. 8. The last three columns indicate the retrieved pressures and the N_2O concentration.

#	Frequency (cm^{-1})	Intensity (cm^{-1}/(molec.cm^{-2}))	Band	Line	P N_2O (mbar)	P total (mbar)	Concentration
1	1150.9099	$4.717.10^{-21}$	$2\nu_2$	P21	48.0 ± 1.2	155.5 ± 6.7	30.8 ± 2.1 %
2	1183.5154	$5.685.10^{-21}$	$2\nu_2$	R17	45.06 ± 0.7	196.0 ± 4.3	23.0 ± 0.9 %
3	1237.8053	$3.802.10^{-21}$	ν_1	P51	48.8 ± 1.8	214.6 ± 12.0	22.7 ± 2.1 %
4	1253.5185	$4.476.10^{-20}$	ν_1	P35	n/a	n/a	n/a

The N_2O concentration retrieved from spectrum number one in Fig. 8 (~30%) is higher than the pre-mixed concentration of ~25%. This difference is within the sample preparation high uncertainty. Spectrum one was recorded 24 hours after the cell had been filled and spectra two and three were recorded following a further 100 hours. All of the measurements very consistently indicate the presence of an air leak into the gas cell. This is clearly confirmed by the increase in retrieved total pressure. During an air leak into the cell one might

#104097 - $15.00 USD Received 17 Nov 2008; revised 20 Dec 2008; accepted 22 Dec 2008; published 24 Dec 2008

also expect the N_2O partial pressure to remain constant, and this was observed in the unchanged values of the retrieved N_2O pressure. The analysis of the concentration retrieval from spectrum four indicates it should be disregarded and the retrieved values were not included in table 1. This is due to spectral saturation of the measured absorption line and the consequential lack of spectral information required for a reliable retrieval. Except for the case of the saturated absorption line, consistency between the retrieved and experimental parameters is good (the main source of discrepancy originating from the sample preparation). These results provide a clear demonstration of the capabilities of the EC-QCL LHR.

5. Retrieval analysis

To characterize the retrieval, the first obvious parameter to consider is χ^2 as defined in Ref. 19. In a well conditioned retrieval, χ^2 should be close to the size of the measurement vector (i.e. the number of datapoints in the experimental spectrum, noted m). It is indeed the case for the broadband absorption and emission retrievals (χ^2/m=0.7). For the high-resolution measurements, χ^2/m is of the order 0.1. This indicates that the measurement noise has been overestimated by a factor 3. This hypothesis is in agreement with the residual observed in Fig. 8. The LO power fluctuations have indeed been observed to be less perturbing during fine frequency scans, improving the detection limit of the EC-QCL LHR to approximately eight times the theoretical shot noise limit. The origin of the noise observed in the broadband scan has been attributed to short cavities (mainly the QCL chip Fabry Perot cavity). During narrow high-resolution frequency scans these effects are minimized by synchronous tuning of all the cavity elements, and consequently residual etalon fringing with a large free spectral range is efficiently suppressed [20].

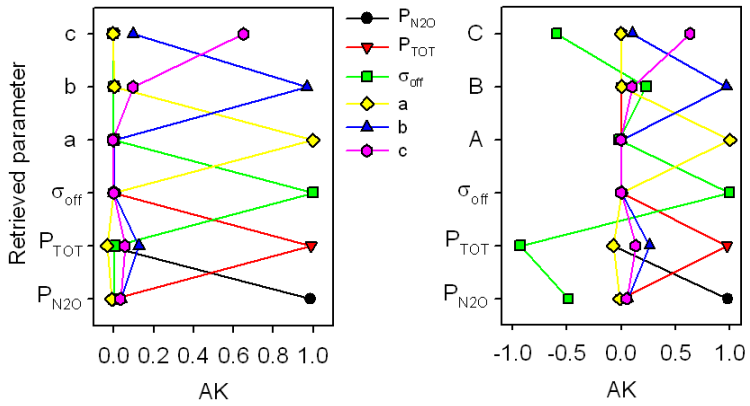

Fig. 9. Averaging kernels from N_2O high-resolution retrievals. The state vector is composed of six elements. The left-hand panel corresponds to retrieval with high confidence, whilst the right-hand panel is typical of a retrieval that should be disregarded.

The averaging kernels (AKs) have been used to further investigate the quality and the relevance of the retrievals. Example AKs are shown in Fig. 9 for two cases: the left-hand panel is typical of a high-quality retrieval producing a result with minimal uncertainty, whilst the right-hand panel shows AKs that indicate the retrieval should be disregarded. In the former all of the retrieved parameters are shown to be almost independent. Specifically the partial pressure of N_2O (P_{N2O}), the frequency offset (σ_{off}), and the constant baseline contribution (a) are fully independent. The total pressure (P_{TOT}) is slightly affected by the linear and quadratic baseline components (b and c), these two components being slightly interdependent as well. In this case one can be confident in the retrieved parameters. In the right-hand plot it is clear that the retrieval of the frequency offset parameter is strongly anti-

#104097 - $15.00 USD Received 17 Nov 2008; revised 20 Dec 2008; accepted 22 Dec 2008; published 24 Dec 2008

correlated to the total pressure, the partial pressure of N_2O, and the quadratic component of the baseline. Therefore in this case confidence in the retrieved parameters is very low and they should be disregarded. In practice, the reliability of the retrievals was found to be mainly affected by the baseline parameters (non-linearity and slope steepness), which depends on the LO power modulation occurring during the laser scan. The integration of this piece of information into the forward model should mitigate this effect.

6. Conclusion

The performance of an EC-QCL LHR tunable over more than 100 cm^{-1} through LO frequency tuning has been demonstrated for both sample emission and transmission modes. To the best of our knowledge this is the first time that thermal IR LHR operation has been achieved over a frequency range of more than 100 cm^{-1}.

Two approaches to the use of a widely tunable LHR have been developed and described: a low spectral resolution sampling mode suitable for characterization of broadband absorbers and emitters, and a high-resolution mode where coarse central frequency tuning over a wide range is combined with fine continuous laser frequency scans.

The system's spectroscopic measurement capabilities have been demonstrated with concentration retrievals of Freon 12 in both transmission and emission modes, as well as concentration retrievals of a N_2O-air mixture at reduced pressure. The measurements combined with an OEM retrieval approach have been analyzed to provide absorber or emitter concentration information with great confidence.

From this first demonstration there are potential improvements to be made, since the excess noise was observed to be twenty-two and eight times the theoretical shot noise limit for the broad and fine scanning modes respectively. Cavity control during broad scanning mode, better mechanical stability of the laser cavity and enhanced laser optical isolation are the first steps toward improved performances of the instrument.

Acknowledgments

DW acknowledges support from the UK NERC Molecular Spectroscopy Facility. GW acknowledges financial support from the MIRTHE NSF Engineering Research Center and co-funding from a DoE STTR grant from Aerodyne Research Inc. The authors are grateful to Gary Williams and Wayne Robins from the RAL Space Science and Technology Department (SSTD) for their technical support. They are also very grateful to Dr. Kevin Smith from SSTD for reading the manuscript and providing most valuable comments.

#104097 - $15.00 USD Received 17 Nov 2008; revised 20 Dec 2008; accepted 22 Dec 2008; published 24 Dec 2008